J. Phys.: Condens. Matter **8** (1996) 2557–2569. Printed in the UK

Plasmon dispersion in A_3C_{60} (A = K, Rb)

O Gunnarsson†, V Eyert†, M Knupfer‡, J Fink‡ and J F Armbruster§

† Max-Planck-Institut für Festkörperforschung, D-70506 Stuttgart, Germany

‡ Institut für Festkörperforschung, IFW Dresden eV, Postfach 270016, D-01171 Dresden, Germany

§ Forschungszentrum Karlsruhe, Institut für Nukleare Festkörperphysik, Postfach 3640, D-76021 Karlsruhe, Germany

Received 10 January 1996

Abstract. We present experimental and theoretical results for the dispersion of the 0.5 eV charge-carrier plasmon in A_3C_{60} (A = K, Rb) compounds. The experimental dispersion in K_3C_{60} is zero within the experimental accuracy, and the theoretical dispersion is slightly negative. We show that the small dispersion results from two large, opposing effects. Local-field effects tend to lead to a large negative dispersion, while interband transitions largely cancel this effect. The interband effects can be thought of in terms of the dielectric function due to classical, polarizable spheres describing the C_{60} molecules. This dielectric function reduces the plasmon energy, and the reduction of the dielectric function with increasing q tends to lead to a large, positive dispersion.

1. Introduction

C_{60} compounds have a plasmon at about 25 eV, corresponding to the oscillation of both the σ- and π-electrons, and another plasmon at about 6 eV, essentially corresponding to the oscillation of the π-electrons. In addition, the doped compounds A_3C_{60} (A = K, Rb) have a third plasmon at about 0.5 eV, corresponding to the oscillation of the three electrons which the alkali atoms have donated into the partly filled t_{1u} band [1]. Interestingly, this plasmon appears to have a negligible dispersion [1], in contrast to the substantial, positive dispersion found for most free-electron-like systems. It has actually been predicted that for a solid consisting of weakly interacting units, like the C_{60} molecules, the dispersion should be large and negative [2].

Here we present new measurements on single-phase K_3C_{60} of the plasmon dispersion, and show that it is indeed very close to zero. We further perform calculations of the plasmon dispersion in the random-phase approximation (RPA) for a tight-binding model of C_{60}, taking into account band-structure and local-field (inhomogeneity) effects. We show that the RPA, when applied to a realistic model of C_{60}, does indeed predict a very small (slightly negative) dispersion.

Anomalously small, or even negative, dispersions have been observed for some alkali metals [3]. It has been shown that in this case the anomalous dispersion is due to interband transitions, and that transitions into unoccupied d states tend to *reduce* the dispersion [4]. Here we show that the effect of the interband transitions for C_{60} is exactly the opposite, and that the interband transitions tend to *increase* the dispersion. The reason is that the interband transitions in this case essentially describe the dielectric function from an array of weakly interacting C_{60} molecules. This dielectric function reduces the plasmon energy.

0953-8984/96/152557+13$19.50 © 1996 IOP Publishing Ltd

For larger values of the wave vector q, the dielectric function is substantially reduced, and therefore the reduction of the plasmon frequency is less important. The result is a tendency of the plasmon energy to increase with q. The effects of the interband transitions is the most important difference from the earlier work of Kresin and Kresin [2], who neglected these transitions and therefore predicted the dispersion to be large and negative.

The importance of the local-field effects for these very inhomogeneous systems have been emphasized by Kresin and Kresin [2], who studied a one-band model with essentially a free-electron dispersion but took the inhomogeneity of the charge density into account. Since the t_{1u} level is threefold degenerate, we here study a three-band model, using a tight-binding model to obtain a fairly realistic description of the band structure and wave functions. The orientational disorder in the real system is neglected. We show how this model can rather accurately be mapped onto a one-band model, as far as the dielectric properties are concerned. We then discuss the local-field effects using a formalism introduced earlier [5]. This formalism has been applied to NiO, where we emphasized the importance of the Coulomb integral describing the self-interaction of the charge density corresponding to a product function involving the important transitions in the dielectric function. For C_{60}, where the t_{1u} orbitals are rather extended, this Coulomb integral is rather small and does not play an important role. The important aspect is instead that the Fourier transform of the t_{1u} charge density decays relatively rapidly with increasing q over the relevant range of q. We demonstrate that this leads to a substantial negative dispersion, which is, however, largely cancelled by the tendency of the interband transitions to give a positive dispersion. The small dispersion is therefore rather nontrivial and results from two fairly large but essentially cancelling effects.

We present the formalism used for the calculations in section 2, the model in section 3 and the experimental and theoretical results in section 4. In section 5 we perform a calculation in the t_{1u} space and analyse the local-field effects and in section 6 we study the dielectric function due to the polarizability of the C_{60} molecules classically. The results are summarized in section 7.

2. Formalism

The plasmon dispersion is determined by the response function, and the formalism for calculating this function is presented below. We essentially follow our earlier work [5, 6]. The RPA has been applied to a free C_{60} molecule by, e.g., Bertsch *et al* [7] and by Alasia *et al* [8]. In the RPA, the irreducible polarizability for the frequency ω is given by

$$P_0(\boldsymbol{r},\boldsymbol{r}',\omega)=2\sum_{\boldsymbol{k}n}\sum_{\boldsymbol{k}'n'}\frac{\psi_{\boldsymbol{k}n}(\boldsymbol{r})\psi^*_{\boldsymbol{k}n}(\boldsymbol{r}')\psi^*_{\boldsymbol{k}'n'}(\boldsymbol{r})\psi_{\boldsymbol{k}'n'}(\boldsymbol{r}')}{\varepsilon(\boldsymbol{k}n)-\varepsilon(\boldsymbol{k}'n')-\omega}[f(\boldsymbol{k}n)-f(\boldsymbol{k}'n')] \tag{1}$$

where $\psi_{\boldsymbol{k}n}(\boldsymbol{r})$ is the wave function for a state with the wave vector $\boldsymbol{k}$, band index n and energy $\varepsilon(\boldsymbol{k}n)$. $f(\boldsymbol{k}n)$ is the Fermi function and a factor 2 comes from summation over spin. The Bloch states $\psi_{\boldsymbol{k}n}(\boldsymbol{r})$ are expressed as

$$\psi_{\boldsymbol{k}n}(\boldsymbol{r})=\frac{1}{\sqrt{N}}\sum_{iL\alpha}\mathrm{e}^{\mathrm{i}\boldsymbol{k}\cdot\boldsymbol{R}_\alpha}c_{iL}(\boldsymbol{k}n)\phi_L(\boldsymbol{r}-\boldsymbol{R}_i-\boldsymbol{R}_\alpha) \tag{2}$$

where $\boldsymbol{R}_i$ gives the positions of the 60 atoms inside a molecule relative to the position $\boldsymbol{R}_\alpha$ of that molecule. $L\equiv(l,m)$ labels the basis functions ϕ_L (e.g., one 2s and three 2p) on a given atom and N is the number of molecules in the system. Later we also use three t_{1u} orbitals as basis functions. In that case there is no sum over $\boldsymbol{R}_i$ and the sum over L refers

to the three t_{1u} basis states. We now introduce a new basis set of product functions for describing the polarizability

$$\Phi_{\boldsymbol{q}iLL'}(\boldsymbol{r}) \equiv \Phi_{\boldsymbol{q}\nu}(\boldsymbol{r}) = \frac{1}{\sqrt{N}} \sum_{\alpha} \mathrm{e}^{\mathrm{i}\boldsymbol{q}\cdot\boldsymbol{R}_\alpha} \phi_L(\boldsymbol{r} - \boldsymbol{R}_i - \boldsymbol{R}_\alpha)\phi_{L'}(\boldsymbol{r} - \boldsymbol{R}_i - \boldsymbol{R}_\alpha) \tag{3}$$

where we have used $\nu \equiv iLL'$ as a combined index. If we assume that the overlap between ϕs on different atoms can be neglected, we obtain

$$P_0(\boldsymbol{r}, \boldsymbol{r}', \omega) = \sum_{\boldsymbol{q}} \sum_{iLL'} \sum_{jL_1L_2} \Phi^*_{\boldsymbol{q}iLL'}(\boldsymbol{r}) \tilde{P}_0(iLL', jL_1L_2, \boldsymbol{q}, \omega) \Phi_{\boldsymbol{q}jL_1L_2}(\boldsymbol{r}') \tag{4}$$

where the sum over $\boldsymbol{q}$ is limited to the first Brillouin zone and

$$\tilde{P}_0(iLL', jL_1L_2, \boldsymbol{q}, \omega) = \frac{2}{N} \sum_{\boldsymbol{k}nn'} \frac{c_{iL}(\boldsymbol{k}n)c^*_{iL'}(\boldsymbol{k}+\boldsymbol{q}n')c^*_{jL_1}(\boldsymbol{k}n)c_{jL_2}(\boldsymbol{k}+\boldsymbol{q}n')}{\varepsilon(\boldsymbol{k}n) - \varepsilon(\boldsymbol{k}+\boldsymbol{q}n') - \omega} \times [f(\boldsymbol{k}n) - f(\boldsymbol{k}+\boldsymbol{q}n')]. \tag{5}$$

In this way we have expressed the irreducible polarizability in terms of matrices with the dimension $60 \times 4 \times 4 = 960$, if there are four basis functions per atom and one C_{60} molecule per unit cell.

We now consider the screening of an external potential

$$V^{ext}(\boldsymbol{r}, t) = V^{ext}(\boldsymbol{r}, \omega)\mathrm{e}^{-\mathrm{i}\omega t} = V^{ext}(\boldsymbol{q}, \omega)\mathrm{e}^{\mathrm{i}(\boldsymbol{q}\cdot\boldsymbol{r}-\omega t)}/\sqrt{N\Omega}. \tag{6}$$

The screened potential, $V^{scr}(\boldsymbol{r}, \omega)$, satisfies the equation

$$V^{scr}(\boldsymbol{r}, \omega) = V^{ext}(\boldsymbol{r}, \omega) + \int \mathrm{d}^3r' \int \mathrm{d}^3r'' v(\boldsymbol{r} - \boldsymbol{r}')P^0(\boldsymbol{r}', \boldsymbol{r}'', \omega)V^{scr}(\boldsymbol{r}'', \omega) \tag{7}$$

where $v(\boldsymbol{r} - \boldsymbol{r}')$ is the unscreened Coulomb interaction. This equation describes how the screened potential induces a charge density P^0V^{scr} and an induced potential vP^0V^{scr}. To solve for V^{scr}, we notice that due to the separable form [9, 10] of P_0 in equation (4), only integrals over $\Phi_{\boldsymbol{q}\nu}(\boldsymbol{r})V^{scr}(\boldsymbol{r}, \omega)$ enter. Thus we introduce

$$\tilde{V}^{scr}_{\nu}(\boldsymbol{q}, \omega) = \int \mathrm{d}^3r \ \Phi_{\boldsymbol{q}\nu}(\boldsymbol{r})V^{scr}(\boldsymbol{r}, \omega) \tag{8}$$

together with a similar definition for $\tilde{V}^{ext}$. We then find

$$\tilde{V}^{scr}_{\nu}(\boldsymbol{q}, \omega) = \tilde{V}^{ext}_{\nu}(\boldsymbol{q}, \omega) + \sum_{\mu,\nu'} \tilde{v}_{\nu\mu}(\boldsymbol{q})\tilde{P}^0_{\mu\nu'}(\boldsymbol{q}, \omega)\tilde{V}^{scr}_{\nu'}(\boldsymbol{q}, \omega) \tag{9}$$

where

$$\tilde{v}_{\mu\nu}(\boldsymbol{q}) = \int \mathrm{d}^3r \ \mathrm{d}^3r' \ \Phi_{\boldsymbol{q}\mu}(\boldsymbol{r})v(\boldsymbol{r} - \boldsymbol{r}')\Phi^*_{\boldsymbol{q}\nu}(\boldsymbol{r}'). \tag{10}$$

We now treat v and P^0 as matrices with indices μ and ν and V^{ext} and V^{scr} as vectors. The solution of equation (9) can be written as

$$\tilde{V}^{scr} = (1 - \tilde{v}\tilde{P}^0)^{-1}\tilde{V}^{ext}. \tag{11}$$

The condition for having a plasmon is that an induced potential can be sustained even when $\tilde{V}^{ext} \equiv 0$. This condition is given by

$$\det(1 - \tilde{v}\tilde{P}^0) = 0. \tag{12}$$

We further write

$$\Phi_{\boldsymbol{q}\mu}(\boldsymbol{r}) = \frac{1}{\sqrt{N\Omega}} \left\{ f_\mu(\boldsymbol{q})\mathrm{e}^{\mathrm{i}\boldsymbol{q}\cdot\boldsymbol{r}} + \sum_{\boldsymbol{G}\neq 0} C_{\boldsymbol{q}+\boldsymbol{G}\mu}\mathrm{e}^{\mathrm{i}(\boldsymbol{q}+\boldsymbol{G})\cdot\boldsymbol{r}} \right\} \tag{13}$$

where Ω is the volume of the unit cell and $\boldsymbol{q}$ is limited to the first Brillouin zone. Here

$$f_\mu(\boldsymbol{q}) = f_{iLL'}(\boldsymbol{q}) = \frac{1}{\sqrt{\Omega}} \int \mathrm{d}^3 r \ \phi_{iL}(\boldsymbol{r})\phi_{iL'}(\boldsymbol{r})\mathrm{e}^{-\mathrm{i}\boldsymbol{r}\cdot\boldsymbol{q}}. \tag{14}$$

If $L = L'$, we obtain that

$$f_{iLL}(\boldsymbol{q} \to 0) = 1/\sqrt{\Omega}$$

from the normalization of $\phi_{iL}(\boldsymbol{r})$. We now consider the matrix element $\tilde{v}_{\mu\nu}(\boldsymbol{q})$ in more detail and write

$$\tilde{v}_{\mu\nu}(\boldsymbol{q}) = f_\mu(\boldsymbol{q})v(\boldsymbol{q})f_\nu(\boldsymbol{q}) + w_{\mu\nu}(\boldsymbol{q}) \tag{15}$$

where $v(q) = 4\pi e^2/q^2$ and

$$w_{\mu\nu}(\boldsymbol{q}) = \sum_{\boldsymbol{G}\neq 0} v(|\boldsymbol{q}+\boldsymbol{G}|)|C_{\boldsymbol{q}+\boldsymbol{G}}|^2. \tag{16}$$

From the definition, it follows that $w_{\mu\nu}(\boldsymbol{q})$ is obtained by constructing the charge density $\Phi_{\boldsymbol{q}\nu}(\boldsymbol{r})$, subtracting the $\boldsymbol{q}$th Fourier coefficient and then calculating the interaction of this charge density with itself.

The local-field effects enter both via the $\boldsymbol{q}$-dependence of $f_{iLL}(\boldsymbol{q})$ and the finite value of $w_{\mu\nu}(q)$. For systems with very localized levels, e.g., NiO treated earlier [5], the important effects come via $w_{\mu\nu}(q)$. Below we show that for C_{60} the important effects come from the reduction of $f_{iLL}(\boldsymbol{q})$ with increasing value of $|\boldsymbol{q}|$.

3. Model

We now introduce a model of C_{60} for which we calculate the plasmon dispersion. We consider the one-particle Hamiltonian describing the states in an isolated molecule

$$H^0_{Mol} = \sum_{iL\sigma} \varepsilon_L n_{iL\sigma} + \sum_{iLjL'\sigma} [t(iL, jL')\psi^\dagger_{iL\sigma}\psi_{jL'\sigma} + \mathrm{HC}] \tag{17}$$

where ε_L gives the energies of the 2s and 2p levels and $t(iL, jL')$ gives the hopping integrals between the states. We use the parameters of Tomanek and Schluter [11], and assume nearest-neighbour hopping as usual [11]. From equation (17) we obtain the levels of an isolated C_{60} molecule and the corresponding molecular orbitals (MO). In the solid these levels are broadened to narrow subbands. We neglect the corresponding dispersion for all the bands, except for the t_{1u} band, which in the doped system is partially occupied. The dispersion of the t_{1u} band is important, since it determines the metallic screening. To obtain the dispersion of the t_{1u} band, we have given a 3×3 analytical $\boldsymbol{k}$-dependent Hamiltonian [14], which is used here. We also neglect the mixing in the solid of MOs with different energies. This mixing is weak, since the energy separation of the MOs is large compared with the hopping matrix elements.

The Coulomb integrals between the orbitals are defined as

$$V(iL\alpha, jL'\beta; mL''\gamma, nL'''\delta) = e^2 \int \mathrm{d}^3 r \int \mathrm{d}^3 r' \ \phi_L(\boldsymbol{r} - \boldsymbol{R}_i - \boldsymbol{R}_\alpha)\phi_{L'}(\boldsymbol{r} - \boldsymbol{R}_j - \boldsymbol{R}_\beta)$$
$$\times \frac{1}{|\boldsymbol{r} - \boldsymbol{r}'|}\phi_{L''}(\boldsymbol{r}' - \boldsymbol{R}_m - \boldsymbol{R}_\gamma)\phi_{L'''}(\boldsymbol{r}' - \boldsymbol{R}_n - \boldsymbol{R}_\delta). \tag{18}$$

Since we neglect the overlap of the functions centred on different atoms, V is nonzero only if $(i\alpha) = (j\beta)$ and $(m\gamma) = (n\delta)$. If $L = L'$ and if $L'' = L'''$, this integral corresponds to the

interaction between two monopoles, which is large. If the two conditions are not fulfilled, the interaction is between multipoles and smaller. We therefore make the assumption

$$V(iL\alpha, jL'\beta; mL''\gamma, nL'''\delta) = \delta_{L,L'}\delta_{L'',L'''}\delta_{i,j}\delta_{\alpha,\beta}\delta_{m,n}\delta_{\gamma,\delta} \times \begin{cases} e^2/|\boldsymbol{R}_i + \boldsymbol{R}_\alpha - \boldsymbol{R}_j - \boldsymbol{R}_\delta| & \text{for } |\boldsymbol{R}_i + \boldsymbol{R}_\alpha - \boldsymbol{R}_j - \boldsymbol{R}_\delta| > 0 \\ V_0 & \text{for } |\boldsymbol{R}_i + \boldsymbol{R}_\alpha - \boldsymbol{R}_j - \boldsymbol{R}_\delta| = 0. \end{cases} \tag{19}$$

This approximation has been discussed elsewhere [6]. For the on-site interaction, we have obtained $V_0 = 12$ eV from atomic calculations [6]. With the approximation (19) it is then straightforward to calculate $\tilde{v}(iLL, jL'L', \boldsymbol{q})$ by using the Ewald technique. The dimension of the matrices in (9) is now reduced to $60 \times 4 = 240$. The approximation (19) means that we neglect the polarization of the individual C atoms, but that we allow for polarization through charge transfer from one atom to another. Since the diameter of the C_{60} molecule is large compared with the size of a C atom, we expect the charge transfer across the molecule to be important. A similar approximation was also used by Bertsch *et al* [7], but their result for the polarizability of the free molecule was less good than the result below, presumably because Bertsch *et al* [7] introduced some additional approximations. In the calculations for the solid, we consider an fcc lattice with the lattice parameter 14.39 Å and one C_{60} molecule per unit cell. The lattice parameter corresponds to Rb_3C_{60}, but the results are not changed very much for the lattice parameter of K_3C_{60}. To be able to perform the calculations, we assume that all molecules have the same orientation, while it is experimentally believed that the molecules take one of two different orientations in a random way [15]. While we consider an ordered system, the true system therefore has a substantial disorder.

In this model we find that the polarizability α of a free C_{60} molecule is 50 Å^3. From the Clausius–Mossotti relation and the experimental dielectric function (4.4) for an undoped C_{60} crystal [12], we deduce a molecular polarizability of 89 Å^3. The difference from our calculated value is probably due to the neglect of the polarizability of the individual C atoms and to the neglect of exchange–correlation effects (using the RPA). To obtain the correct dielectric function of the undoped system within our model, we have expanded the C_{60} molecule by 23%. This is somewhat smaller than the expansion 33% deduced by Yannouleas and Landman, who considered the effective capacitance of C_{60} [16]. The resulting plasmon energy is somewhat too large compared with experiment, and we have therefore reduced the theoretical t_{1u} band width given by the analytical Hamiltonian [14] by a factor 0.6. These corrections are not essential for the behaviour of the dispersion.

4. Results

In figure 1 we show the experimental results for the electron loss function as a function of the energy and momentum transfer for K_3C_{60}. The data are normalized to the intensity of the volume plasmon at about 25 eV. These results were obtained by electron energy-loss spectroscopy (EELS) measurements in transmission using a 170 keV spectrometer [17]. The energy and momentum resolution were chosen to be 120 meV and 0.05 Å^{-1}, respectively. Single-phase K_3C_{60} films were grown using vacuum distillation [18, 19]. The film thickness was about 1500 Å. Details of the sample preparation and characterization are given elsewhere [20]. The raw data have been corrected for elastic line contributions. We note that this procedure did not alter the energy position of the plasmon at 0.5 eV in figure 1. The plasmon peak position is independent of q within the experimental accuracy, implying a very small dispersion of the plasmon. The peak at about 1.3 eV is due to an interband $t_{1u} \rightarrow t_{1g}$ transition. Intriguingly, the width of the plasmon is also independent of

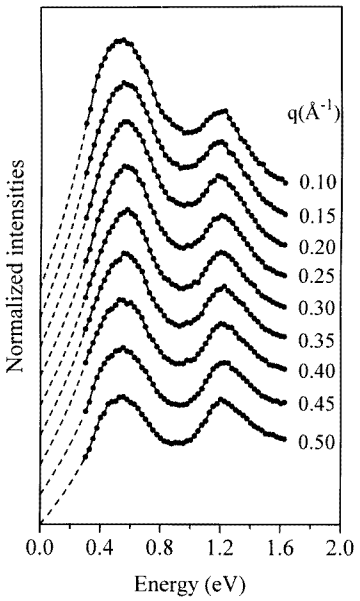

Figure 1. The experimental loss function for K_3C_{60} as a function of energy and for different values of the momentum transfer. The dashed lines indicate the energy region where the curves have been extrapolated to zero energy after elastic line subtraction.

the momentum transfer and it is furthermore about as large as the plasmon energy itself. In simple metals the plasmon width is mainly determined by a decay into interband transitions. However, the first interband transition at about 1.3 eV is much higher than the plasmon energy and the transitions inside the t_{1u} band are probably at too low energies to explain the large, symmetric broadening of the plasmon. The origin of this broadening will be discussed in a separate publication [21].

In figure 2 we show the calculated plasmon energy for $\boldsymbol{q}$ in different directions. In agreement with experiment, the theoretical dispersion is small. The weak direction dependence may be a defect of performing the calculations for an ordered crystal.

To analyse the results, we have further performed a calculation where all the interband transitions are suppressed, and only transitions within the t_{1u} band are allowed. The results are also shown in figure 2. It is striking that the dispersion is now strongly negative. For $q = 0$ the plasmon energy is reduced by about a factor of two by the interband transitions. The reason is that these transitions essentially describe the dielectric function ($\epsilon \sim 4$) of the undoped C_{60} compound, neglecting the fact that the available interband transitions differ somewhat for the doped solid due to the partial filling of the t_{1u} band. This dielectric function reduces the plasmon energy by a factor of $\sqrt{\epsilon}$. For larger values of q, however, the interband transitions apparently do not reduce the plasmon energy very much. These results are analysed below.

5. Calculation within the t_{1u} space

Above we have illustrated that if only the t_{1u} orbitals are considered, the dispersion is negative. In this section we want to analyse this in detail. For this reason we now present a simplified calculation, while the results in figure 2 were obtained using the full formalism in section 2.

In the analysis below, the basis functions $\phi_L(\boldsymbol{r} - \boldsymbol{R}_i - \boldsymbol{R}_\nu)$ in equation (2) refer to the three t_{1u} orbitals, and $\boldsymbol{R}_i = 0$. There are six functions $\Phi_{LL'}(\boldsymbol{r})$ (equation (3)),

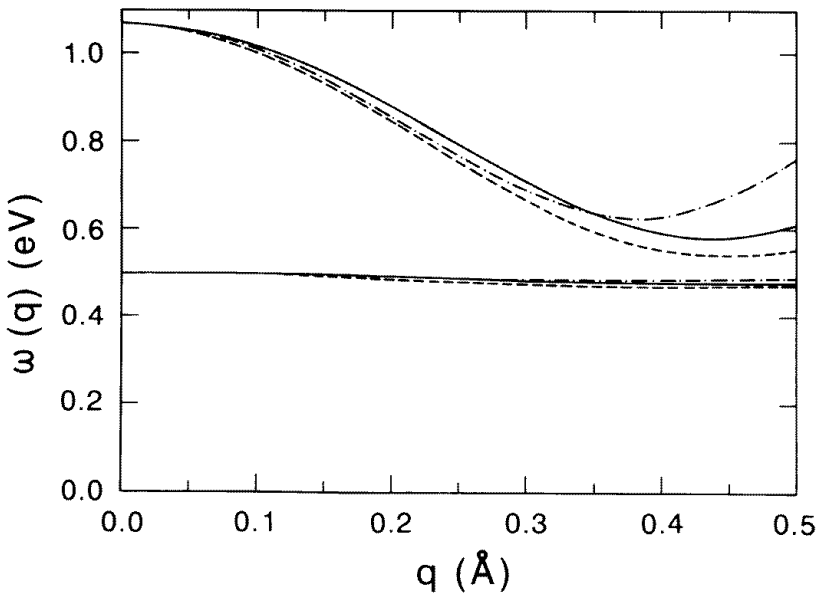

Figure 2. The theoretical plasmon energy as a function of $|\boldsymbol{q}|$ for different directions ((1, 0, 0) (full line), (1, 1, 0) (dashed line) and (1, 1, 1) (chain line)) of $\boldsymbol{q}$. The upper curves (in the energy range 0.55–1.07 eV) show calculations in the t_{1u} space and the lower curves (energy range 0.47–0.50 eV) show results of the full calculation, including interband transitions.

corresponding to $LL' = (1,1)$, $(2,2)$, $(3,3)$, $(1,2)$, $(2,3)$ and $(3,1)$. These functions are labelled by $\nu = 1, \ldots, 6$. The functions $(2,1)$, $(3,2)$ and $(1,3)$ are identical to the ones already considered. For $|\boldsymbol{q}| \to 0$, the functions $f_{LL'}(\boldsymbol{q}) \to \delta_{LL'}/\sqrt{\Omega}$. The matrix elements $\tilde{v}_{\mu\nu}$ of the Coulomb interaction (equation (15)) are therefore large only if $L = L'$. The corresponding values are then very similar. We introduce the approximation that these matrix elements have the same value (v_0) and that all the other matrix elements of $\tilde{v}$ are zero. The 6×6 matrix $\tilde{v}_{\mu\nu}$ then takes the approximate form

$$\tilde{v} \approx \begin{pmatrix} v_0 & v_0 & v_0 & 0 & 0 & 0 \\ v_0 & v_0 & v_0 & 0 & 0 & 0 \\ v_0 & v_0 & v_0 & 0 & 0 & 0 \\ 0 & 0 & 0 & 0 & 0 & 0 \\ 0 & 0 & 0 & 0 & 0 & 0 \\ 0 & 0 & 0 & 0 & 0 & 0 \end{pmatrix}. \tag{20}$$

The complete neglect of all elements but the ones in the upper left corner is by itself not quite justified, but becomes justified in the context where $\tilde{v}$ is used below. We also need an approximation for the polarizability $\tilde{P}^0(LL', L_1L_2, \boldsymbol{q}, \omega)$. From the definition in equation (5), we can see that if $L = L_1$ and $L' = L_2$, the numerator takes the form $|c_L(\boldsymbol{k}n)c_{L'}(\boldsymbol{k} + \boldsymbol{q}n')|^2$. Since this quantity is always positive, there is no cancellation between terms with different $\boldsymbol{k}$ and nn'. These matrix elements are therefore important. For small values of q the elements with $L = L'$ and $L_1 = L_2$ are also large. We therefore

make the approximation

$$\tilde{P}_0 \approx \begin{pmatrix} p_0 & p_1 & p_1 & 0 & 0 & 0 \\ p_1 & p_0 & p_1 & 0 & 0 & 0 \\ p_1 & p_1 & p_0 & 0 & 0 & 0 \\ 0 & 0 & 0 & p_2 & 0 & 0 \\ 0 & 0 & 0 & 0 & p_2 & 0 \\ 0 & 0 & 0 & 0 & 0 & p_2 \end{pmatrix}. \tag{21}$$

We now apply the condition of equation (12) for a plasmon

$$0 = \det(1 - \tilde{v}\tilde{P}^0) = 1 - 3v_0(p_0 + 2p_1) \equiv 1 - 3v_0 p_s. \tag{22}$$

We have thus turned our three-band model into effectively a one-band model, with the polarizability $p_s = p_0 + 2p_1$. We have tested the approximations above, by comparing the dispersion deduced from equation (22) with the dispersion from the full calculation in the t_{1u} space. The difference is at most about 5% and usually much smaller. To proceed further, we now replace the wave functions $\phi_L(\boldsymbol{r})$ by the approximate wave function [2]

$$\phi_L(\boldsymbol{r})^2 = \frac{1}{4\pi R_0^2}\delta(|\boldsymbol{r}| - R_0) \tag{23}$$

where we have assumed that the wave function is uniformly spread out over a shell with the radius $R_0 \approx 3.5$ Å, defined by the nuclear positions in the C_{60} molecule. We then obtain

$$f_{LL}(\boldsymbol{q}) = \frac{1}{\sqrt{\Omega}}\frac{\sin(|\boldsymbol{q}|R_0)}{|\boldsymbol{q}|R_0}. \tag{24}$$

The Coulomb interaction $w_{LL,L'L'}(\boldsymbol{q} = 0)$ is approximately given by

$$w_{LL,L'L'}(\boldsymbol{q} = 0) \approx \frac{e^2}{R_{WS}}\left[\frac{R_{WS}}{R_0} + \left(\frac{R_0}{R_{WS}}\right)^2 - \frac{9}{5}\right] \tag{25}$$

where $R_{WS} \approx 5.6$ Å, is the Wigner–Seitz radius of a C_{60} molecule. From the full calculations we derive $w(0) = 0.45$ eV, in good agreement with the estimate (0.47 eV) in equation (25). We write

$$\tilde{v}_{LL,L_1L_1}(q) = \frac{1}{\Omega}\frac{4\pi e^2}{q^2}\left[1 - (qR_{WS})^2\left(\frac{3}{5} - \frac{1}{3}\frac{R_{WS}}{R_0}\right) + \mathrm{O}(q^4)\right] \tag{26}$$

We further write

$$p_s(\boldsymbol{q}, \omega) = \frac{A + B|\boldsymbol{q}|^2}{\omega^2}|\boldsymbol{q}|^2 \tag{27}$$

which is valid for the values of ω of interest here. Here A and B are constants. There is no contribution of the order $|\boldsymbol{q}|^0$ due to phase-space arguments. We can then write the condition (equation (22)) for a plasmon as

$$0 = 1 - 3p_s v_0 \tag{28}$$

$$= 1 - \frac{12\pi e^2 A}{\omega^2\Omega}\left\{1 + \left[\frac{B}{A} - \frac{1}{5}(R_{WS})^2\left(1 - \frac{5}{9}\frac{R_{WS}}{R_0}\right)\right]|\boldsymbol{q}|^2\right\}. \tag{29}$$

The dispersion is then determined by the coefficient of the $|\boldsymbol{q}|^2$-term. If this coefficient is negative, the dispersion is also negative.

Alternatively, we can write

$$\tilde{v}_{LL,L'L'}(\boldsymbol{q}) = \sum_\alpha \mathrm{e}^{\mathrm{i}\boldsymbol{q}\cdot\boldsymbol{R}_\alpha}\int \phi_L^2(\boldsymbol{r})v(\boldsymbol{r} - \boldsymbol{r}')\phi_{L'}^2(\boldsymbol{r} - \boldsymbol{R}_\alpha)\ \mathrm{d}^3r\ \mathrm{d}^3r'. \tag{30}$$

Using the form (23) for ϕ_L^2, $\tilde{v}$ is the interaction between spherical shells of charges on each site. Since the interaction between two spherical, nonoverlapping charges can be replaced by the interaction between two point charges at the centres of the spheres, we obtain

$$\tilde{v}_{LL,L'L'}(\boldsymbol{q}) = \sum_{\alpha \neq 0} \frac{\mathrm{e}^{\mathrm{i}\boldsymbol{q}\cdot\boldsymbol{R}_\alpha}}{|\boldsymbol{R}_\alpha|} + \frac{e^2}{R_0}. \tag{31}$$

The sum is then independent of R_0 and only the on-site interaction e^2/R_0 depends on the size of the molecules. We replace the sum by an integral

$$\begin{aligned}\tilde{v}_{LL,L'L'}(\boldsymbol{q}) &= \frac{e^2}{\Omega}\int_{|\boldsymbol{r}|>R_{WS}} \mathrm{d}^3 r\ \frac{\mathrm{e}^{\mathrm{i}\boldsymbol{q}\cdot\boldsymbol{r}}}{|\boldsymbol{r}|} + \frac{e^2}{R_0} \approx \frac{1}{\Omega}v(q) - \frac{2\pi e^2}{\Omega}R_{WS}^2 + \frac{e^2}{R_0} \\ &= \frac{1}{\Omega}v(q)\left[1 - \frac{1}{2}(qR_{WS})^2\left(1 - \frac{2}{3}\frac{R_{WS}}{R_0}\right)\right].\end{aligned} \tag{32}$$

We can see that the sum over α in equation (31) is equal to $v(q)/\Omega$, which is what we would obtain if all local-field effects were neglected, minus a correction term. Numerical calculations for a fcc lattice show that this correction term is underestimated by about 20% in the approximation above. If expression (32) is corrected correspondingly, it becomes very similar to expression (26).

It is now immediately clear that if the radius R_0 of the molecule is sufficiently large, the term e^2/R_0 is not sufficient to compensate for the correction term discussed above, and the interaction is *weaker* than if the local-field effects had been neglected. In particular, the relative deviation from the case without local-field effects grows with q, as is indicated by the negative coefficient of q^2 in equation (32). This weaker interaction tends to reduce the dispersion or even lead to a negative dispersion. This applies to C_{60}. On the other hand, if R_0 is small, the interaction is *stronger* than in the case without local-field effects, which then tends to make the dispersion more positive (or less negative). In our earlier work on NiO, the latter case was applicable, because of the very localized nature of the Ni 3d orbital. In that case we focused on the self-interaction $w(0)$ and neglected the effects of $f(\boldsymbol{q})$ in the qualitative discussions.

In the expression (28), we find that the term $B/A \approx -4$ Å^2 and the next term is about -2 Å^2. The coefficient of the $|\boldsymbol{q}|^2$-term is then -6 Å^2. This gives the plasmon energy $\omega(q) \approx \omega(q = 0)(1 - 3q^2)$. This dispersion is a bit smaller than the direction-dependent dispersion derived from the full calculation in the t_{1u} space (the upper curve in figure 2). We observe that in a free-electron-like system the value of B/A is positive. The large, negative value of B/A obtained here is a result of the completely different band structure obtained for an ordered C_{60} solid. We have performed a calculation for disordered, solid C_{60}, considering intraband effects only, as in this section [21]. We then found that the dispersion remains negative, but that it is somewhat less negative than in the ordered solid [21].

6. Interband transitions

Above we showed that the interband transitions lead to a strong reduction of the plasmon energy for small values of $|\boldsymbol{q}|$ while the reduction is small at the zone boundaries. The interband transitions describe how the C_{60} molecules polarize as a response to the oscillations of the t_{1u} electrons. To understand this effect better, we treat the C_{60} molecules as classical polarizable spheres. This does not include the metallic screening, which was already taken into account in the calculation within the t_{1u} space, but includes the essential effects of the interband transitions.

For simplicity we first replace the C_{60} molecules by metallic spheres, with the radii R. Since the polarizability of such a sphere is R^3, we choose $R = 4.46$ Å, to reproduce the polarizability 89 Å^3 of a free C_{60} molecule. It is interesting that this radius is larger than the radius, $R_0 = 3.5$ Å, of the C_{60} molecule defined by the position of the nuclei plus the covalent radius, 0.7 Å, of a C atom. This illustrates that the outermost tails of the atomic charge distribution play an important role for the polarizability. This effect was neglected in our calculation of the molecular polarizability, since we did not allow for a polarization of the individual atoms. Our expansion of the C_{60} molecules, however, probably describes most of this effect.

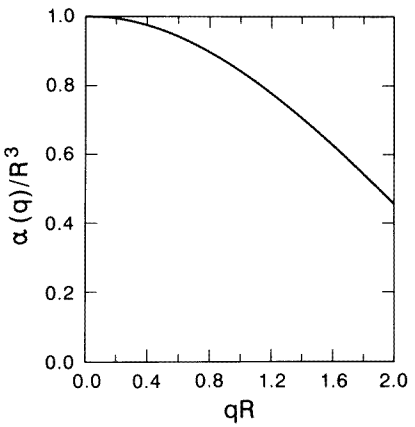

Figure 3. The molecular polarizability $\alpha(q)$ (equation (36)) for a metallic sphere as a function of qR, where R is the sphere radius. In the $(1, 0, 0)$ direction, the Brillouin zone boundary corresponds to $qR = 1.95$.

We first calculate the induced dipole moment when an external, longitudinal electric field

$$\boldsymbol{E}^{ext}(\boldsymbol{r}) = E^{ext}\hat{\boldsymbol{z}}\mathrm{e}^{\mathrm{i}qz} \tag{33}$$

with a finite vector $\boldsymbol{q} = (0, 0, q)$ is applied to the sphere. For simplicity we have assumed that the field is in the z-direction. This field is created by an external charge

$$\rho_{ext}(\boldsymbol{r}) = \frac{1}{4\pi}\boldsymbol{\nabla}\cdot\boldsymbol{E}^{ext} = \frac{\mathrm{i}}{4\pi}E_0 q\mathrm{e}^{\mathrm{i}qz}. \tag{34}$$

To obtain the induced field outside the sphere we create the images of the external charges in the sphere. The dipole in the z-direction of the image charges is then

$$P(q) = \int_{|r|>R}\mathrm{d}^3\, r\left(-\frac{\mathrm{i}}{4\pi}E_0 q\mathrm{e}^{\mathrm{i}qz}\frac{R}{r}\right)\frac{zR^2}{r^2}. \tag{35}$$

We then find the dipole polarizability

$$\alpha(q) = \frac{P(q)}{E^{ext}} = -R^3\int_{qR}^{\infty}\frac{\mathrm{d}r}{r}\left(\cos r - \frac{1}{r}\sin r\right). \tag{36}$$

All higher multipole moments are neglected, which is consistent with the treatment below. In the limit of $q = 0$ the polarizability reduces to R^3, as it should. In figure 3 we show the dependence of $\alpha(q)$ on qR. At q-values corresponding to the Brillouin zone boundaries, $\alpha(q)$ is reduced by about a factor of two.

We now consider the response of C_{60} molecules on a fcc lattice to an external $\boldsymbol{q}$-dependent electric field, following the Lorentz–Lorentz approach for $\boldsymbol{q} \to 0$. As in this approach we consider the C_{60} molecules as point dipoles. The finite size of the molecules

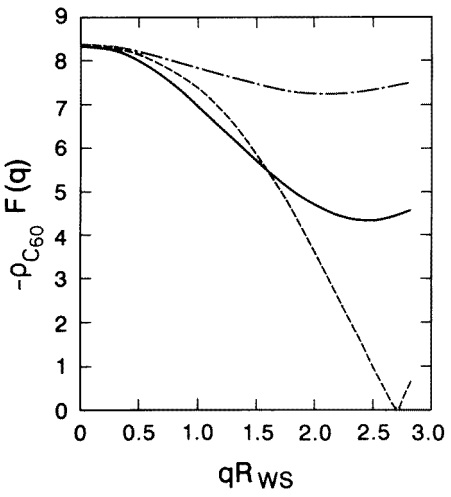

Figure 4. The function $-\rho_{C_{60}}F(\boldsymbol{q})$ in equation (39) as a function of qR_{WS}, where R_{WS} is the Wigner–Seitz radius, for the directions (1, 0, 0) (full curve), (1, 1, 0) (dashed curve) and (1, 1, 1) (chain curve). In the (1, 0, 0) direction the Brillouin zone boundary corresponds to $qR_{WS} = 2.5$.

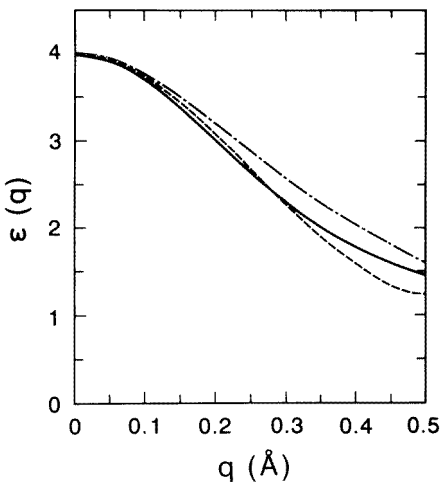

Figure 5. The dielectric function in equation (43) as a function of q, for the directions (1, 0, 0) (full curve), (1, 1, 0) (dashed curve) and (1, 1, 1) (chain curve). In the (1, 0, 0) direction the Brillouin zone boundary corresponds to $q = 0.44$.

has, however, been included in the q-dependence of the molecular dipole polarizability, as discussed above. The neglect of higher multipoles is only used for the purpose of the present analysis, while in the full calculation of the results in figure 2 such an approximation is not used. We apply the external, longitudinal field

$$\boldsymbol{E}_{\nu}^{ext} = \boldsymbol{E}^{ext}\mathrm{e}^{\mathrm{i}\boldsymbol{q}\cdot\boldsymbol{R}_{\nu}} \tag{37}$$

to the molecule at the position $\boldsymbol{R}_{\nu}$. This field is screened self-consistently, resulting in the induced dipoles $\boldsymbol{p}^{ind}\exp(\mathrm{i}\boldsymbol{q}\cdot\boldsymbol{R}_{\nu})$ and induced fields $\boldsymbol{E}^{ind}\exp(\mathrm{i}\boldsymbol{q}\cdot\boldsymbol{R}_{\nu})$. We then have that

$$\boldsymbol{E}^{ind} = \boldsymbol{p}^{ind}F(q), \tag{38}$$

where

$$F(\boldsymbol{q}) = \frac{1}{\rho_{C_{60}}}\sum_{\nu\neq 0}\left[3\frac{(\hat{\boldsymbol{p}}\cdot\boldsymbol{R}_{\nu})\boldsymbol{R}_{\nu}}{|\boldsymbol{R}_{\nu}|^5} - \frac{\hat{\boldsymbol{p}}}{|\boldsymbol{R}_{\nu}|^3}\right]\mathrm{e}^{\mathrm{i}\boldsymbol{q}\cdot\boldsymbol{R}_{\nu}} \tag{39}$$

where $\rho_{C_{60}}$ is the density of C_{60} molecules, and $\hat{\boldsymbol{p}} = \hat{\boldsymbol{q}}$ is the direction of $\boldsymbol{p}^{ind}$. As in the Lorentz–Lorentz treatment we now write the macroscopic dielectric function as

$$\frac{1}{\epsilon} = 1 + \frac{|\boldsymbol{E}^{ind}|}{|\boldsymbol{E}^{ext}|} + \frac{|\boldsymbol{E}^{self}|}{|\boldsymbol{E}^{ext}|} \tag{40}$$

where for

$$\boldsymbol{E}^{self} = -\frac{4\pi}{3}\rho_{C_{60}}\boldsymbol{p}^{ind} \tag{41}$$

we have used the average over the unit cell of the field from the dipole in that unit cell, as in the Lorentz–Lorentz $q = 0$ treatment. We have here used the value of $\boldsymbol{E}^{ind}$ at the position of a molecule instead of its average over the cell. Furthermore we have

$$\boldsymbol{p}^{ind} = \alpha(q)(\boldsymbol{E}^{ext} + \boldsymbol{E}^{ind}). \tag{42}$$

This leads to

$$\epsilon = \frac{1 - \rho_{C_{60}} F(q)\alpha(q)}{1 - 4\pi\rho_{C_{60}}\alpha(q)/3}. \tag{43}$$

We find $F(0) = 8\pi/3$, which leads to the Clausius–Mossotti relation for $q = 0$. In figure 4 we show the variation of $F(\boldsymbol{q})$. For a q corresponding to the Brillouin zone boundary, F is substantially reduced for the $(1, 0, 0)$ direction, close to zero for the $(1, 1, 0)$ direction but little reduced for the $(1, 1, 1)$ direction. In figure 5 we show the corresponding variation of the dielectric function ϵ. For $\boldsymbol{q} = 0$ and for the lattice parameter used here, the dielectric function is about 4.0 and the plasmon energy is reduced by a factor $\sqrt{\epsilon} = 2.0$. On the other hand, at the Brillouin zone boundaries the dielectric function is close to one, and the plasmon energy is only reduced by a small amount, in agreement with the full calculation. The calculation of the $\epsilon(\boldsymbol{q})$ further correctly predicts that the reduction is largest for the $(1, 1, 1)$ direction and smallest for the $(1, 1, 0)$ direction.

7. Summary

We have presented experimental and theoretical results for the plasmon dispersion in A_3C_{60}, showing that the dispersion is anomalously small. We have demonstrated that this small dispersion is due to two large, almost cancelling effects. Local-field effects tend to give a negative dispersion and interband transitions tend to give a positive dispersion.

We have analysed the effects of the interband transition in terms of a classical dielectric function, treating the C_{60} molecules as metallic spheres. The dielectric function reduces the plasmon energy by a factor $\sqrt{\epsilon}$, which is of the order two for small q but of the order of 1.3 at the Brillouin zone boundaries. To obtain this q-dependence we first studied the induced dipole moment for a free sphere in an external field with a finite q-vector, and found a reduction by almost a factor of two for q at the zone boundary. We then performed an analysis where the C_{60} molecules were treated as point dipoles, along the lines of the Lorentz–Lorentz approach, but considering finite q. We found that the relevant lattice sum depends strongly on the direction and might be reduced by about a factor of two at the zone boundary. As a result, the dielectric function was reduced by about a factor 2.5 at the zone boundary from its value at $q = 0$, resulting in a large tendency to a positive dispersion.

The local-field effects were analysed in a framework where the Fourier transform f of the t_{1u} molecular orbital enters as an important quantity. A second important quantity is the Coulomb self-interaction w of the charge density from a t_{1u} orbital minus its average over the unit cell. We found that f favours a negative dispersion while w favours a positive dispersion. For systems where the relevant orbital is well localized, e.g., the 3d orbital in 3d compounds, w plays the essential role. C_{60} compounds fall at the opposite limit, where f is much more important that w.

Finally, we observe that it would be interesting to study doped, molecular solids where the relative importance of f, w and the dielectric function for the undoped solid is different, and where different types of plasmon dispersions may therefore be observed.

Acknowledgments

This work was supported in part by the European Community Human Capital and Mobility programme through contract No CHRX-CT93-0337.

References

[1] Sohmen E, Fink J and Krätschmer W 1992 *Europhys. Lett.* **17** 51
[2] Kresin V V and Kresin V Z 1994 *Phys. Rev.* B **49** 2715
[3] vom Felde A, Sprösser-Prou J and Fink J 1989 *Phys. Rev.* B **40** 10 181
[4] Aryasetiawan F and Karlsson K 1994 *Phys. Rev. Lett.* **73** 1679
[5] Aryasetiawan F, Gunnarsson O, Knupfer M and Fink J 1994 *Phys. Rev.* B **50** 7311
[6] Gunnarsson O, Rainer D and Zwicknagl G 1992 *Int. J. Mod. Phys.* B **6** 3993
[7] Bertsch G F, Bulgac A, Tomanek D and Wang Y 1991 *Phys. Rev. Lett.* **67** 2690
[8] Alasia F, Broglia R A, Roman H E, Serra Ll, Colo G and Pacheco J M 1994 *J. Phys. B: At. Mol. Phys.* **27** L643
[9] Hayashi E and Shimizu M 1969 *J. Phys. Soc. Japan* **26** 1396
Sinha S K 1969 *Phys. Rev.* **177** 1256
[10] Sham L J 1972 *Phys. Rev.* B **6** 3584
Hanke W 1973 *Phys. Rev.* B **8** 4585
Hanke W and Sham L J 1975 *Phys. Rev.* B **12** 4501
[11] Tomanek D and Schluter M A 1991 *Phys. Rev. Lett.* **67** 2331
[12] Hebard A F, Haddon R C, Flemming R M and Kortan R 1991 *Appl. Phys. Lett.* **59** 2109
[13] Gunnarsson O, Satpathy S, Jepsen O and Andersen O K 1991 *Phys. Rev. Lett.* **67** 3002
[14] Satpathy S, Antropov V P, Anderson O K, Jepsen O, Gunnarsson O and Liechtenstein A I 1992 *Phys. Rev.* B **46** 1773
[15] Stephens P W, Mihaly L, Lee P L, Whetten R L, Huang S M, Kaner R, Deiderich F and Holczer K 1991 *Nature* **351** 632
[16] Yannouleas C and Landman U 1994 *Chem. Phys. Lett.* **217** 175
[17] Fink J 1989 *Adv. Electron. Electron Phys.* **75** 121
[18] Poirier D M 1964 *Appl. Phys. Lett.* **64** 1356
[19] Knupfer M, Poirier D M and Weaver J H 1994 *Phys. Rev.* B **49** 8464
[20] Knupfer M, Fink J, Armbruster J F and Romberg H A 1995 *Z. Phys.* B **98** 9
[21] Liechtenstein A I, Gunnarsson O, Knupfer M, Fink J and Armbruster J F 1996 to be published